PERFORMANCE ANALYSIS OF THREE PORT FULL BRIDGE CONVERTER FOR HYBRID PHOTOVOLTAIC/BATTERY MANAGEMENT SYSTEM

by

Mehmet Akif SENOL

Department of Electrical and Electronics Engineering, Faculty of Engineering and Architecture,
Istanbul Gelisim University, Istanbul, Turkey

Original scientific paper
https://doi.org/10.2298/TSCI180925332S

In this paper, performance analysis of three port full bridge converter based hybrid photovoltaic (PV)/battery management system is explained. The overall control system of the three port full bridge converter based PV/battery management system is created and simulated using MATLAB. Maximum power point tracking of solar PV system is controlled by perturb and observe method. Load regulation of PV/ battery management system is controlled by phase shift pulsewidth modulation technique. The system is tested for various real time operating conditions of the power system such as variation of PV panel voltage, change of battery voltage, and change of load power. The experimental verification also is carried out for developed system. Finally, simulation result and experimental result are compared for the developed system.

Key words: *three port converter, hybrid power system, load regulation, pulsewidth modulation, phase shifting pulsewidth modulation*

Introduction

Hybrid power resources are the hopeful eco-friendly power sources for the future. Hybrid power energy systems (HPES) offer constant and consistent energy supply to the customers [1, 2]. Advanced power switched converters are the primary power modulating devices in HPES. But, the traditional HPES use separate power switched converter for each input energy sources. Therefore conventional HPES consist of several modulators, which derive themselves the demerits of, complicated system circuits, large number of switching elements, large power switching losses, bulky and costly. Multi energy source converters (MESC), also known as multi-port switching converter (MPSC), have been developed to the overcome this disadvantages of the traditional HPES. An MPSC consists of various renewable power energy sources in a single power modulating structure [3-8]. It offers the merits of compressed structure, simple circuit network, high stability, universal control and less fabrication cost and size [9-16].

In [3], a common approach to develop the multiport converters has been explained. First it presents the fundamental DC-DC converter structures such as boost, buck, boost/buck, cuk, zeta and SEPIC converters. In [4], systematic approach to develop multiport converters forms the use of basic pulsating sources cells. Using pulsating source cells, two categories of multiport converters are developed. In the first category of multiport converters, all the input

Author's e-mail: masenol@gelisim.edu.tr

energy sources could deliver the load concurrently or independently. In the second category of multiport converters, only one energy source is permitted to transfer power to load at a time. In [5], introduces a very general topology of multiport converter with DC link and magnetic coupling. Then a three-port converter is taken as an example and different topologies of three-port converter are derived from the general topology. The author thus gives a method to derive different topologies like DC link, magnetically coupled, combination of the both, current fed ports for a typical three-port converter. In [6], presents the static and dynamic analysis of multiport converters. The continuous averaged model of the multiport converter circuit is also presented. In [7], discussion on the selection of suitable topologies of multiport converters for any particular application. It gives set rules to identify the feasible topologies of multiport converters. In [8], presents the modeling of single diode PV arrays circuit model of a PV cell. It discusses design of PV with exhaustive equations governing the mathematical model of a PV array in simulink and explains all the terms regarding the design of the panel. With a practical panel being considered using the datasheet, it brings out the results on the characteristics of the PV panel model. It also includes the characteristics due to changes in the surrounding environmental conditions such as solar irradiation level and temperature level changes. In [9], presents a brief on the modeling of the single diode PV array model. It brings out the characteristics of the PV panel model due to changes in surrounding environmental conditions such as irradiation level and temperature level and also changes in the model parameters such as the diode parameters, variations in panel series and shunt resistances. It also presents an experimental set-up to validate the characteristics and an maximum power point tracking (MPPT) based on incremental conductance method. In [10], presents a typical three-port converter developed from full bridge converter structure. It uses only one full bridge converter to integrate three ports. The three port converter has been taken for a typical hybrid PV/battery system. It thus includes two unidirectional and one bidirectional storage port. Two autonomous control variables are identified to closely regulate flow of power between two ports and the third port provides power balance. A complete power management system which includes MPPT at the PV port and voltage regulation at the load port is also discussed. In [11], describe the new DC link topology of three-port converter for hybrid PV/battery/fuel cell (FC) application. It provides the complete switching state analysis of the converter during different operating modes of operation like with and without battery connected. It also gives a clear procedure to the dynamic modeling of the proposed converter. In [12], a new DC link topology of four port converter for hybrid renewable energy applications. It discusses the modeling of the individual components such as the fuel cell, PV panel, battery and the converter. It presents a structure for the power management system using pulsewidth modulation (PWM) technique. In [13], presents a new DC link topology of three-port converter employing zero voltage switching (ZVS). It gives a very useful explanation on the modes of operation of the converter during single and dual power supply situations, with the help of equivalent circuits in each mode and waveforms. In [14], presents a topology of three port converter employing bidirectional half bridge converters at all the three ports and hence the name triple half-bridge converter. It gives the modes operation of the converter and the control scheme using PWM plus phase shift control. It also provides the structure for the proposed control system and it presents the experimental validation also. In [15], presents an fully isolated topology of three port converter with two input ports are current fed. It uses multi winding transformer for fully provides the operating modes of the current fed converter and also the control principle based on PWM plus phase shift.

In this paper, load voltage regulation of three-port full bridge converter based hybrid PV/battery power system is analyzed. The three port converter integrates two input points and a load points. The topology of the three-port converter used in this application is developed from

full-bridge converter structure, hence referred to as three port full-bridge converter. This topology comes under partially isolated classifications of the converter topologies. The transformer provides isolation to the load port alone and the two input ports are at a common ground. Objective of this paper is given as follows, simulink model of the three port full bridge converter which integrates a PV energy, a battery energy device and the load are developed using MATLAB/SIMULINK toolbox. In this work, centralized control structure for the converter which includes MPPT for the PV source and phase shifting algorithm for load voltage regulation. The power flow analysis of the converter in close loop with variations in panel voltage, variations in battery voltage and variations in load condition are explained. Real time hardware implementation of three port full-bridge converter based hybrid PV/battery management system. Also comparison of simulation and hardware results for different operating modes are explained.

Power flow analysis of the three port full bridge converter based hybrid PV/battery management system

In this section power flow analysis of the closed loop control of three port full bridge converter based hybrid PV/battery management system is presented. A closed loop structure is developed for load voltage regulation and the power analysis for the system with load regulation is presented for different cases, such as variations in panel voltage, battery voltage, and varying load condition. The circuit diagram of three port full bridge converter is shown in fig. 1. Three port full bridge converter consists of a full-bridge converter, at the primary of the high frequency transformer, integrating PV source and battery. The full-bridge consists of two switching legs. The first leg with switches S_{A1} and S_{A2} connects the PV source and the second leg with switches S_{B1} and S_{B2} connects the battery to the transformer. The secondary of the transformer feeds the load after rectification using high frequency diode bridge rectifier and L-C filter.

For the three port full bridge converter shown in fig. 1, we have four switching states (I-IV) available in a turn ON/OFF cycle. The ON/OFF position of the switches, equivalent circuit and equations for each switching state are detailed as follows with respect to the fig. 2.

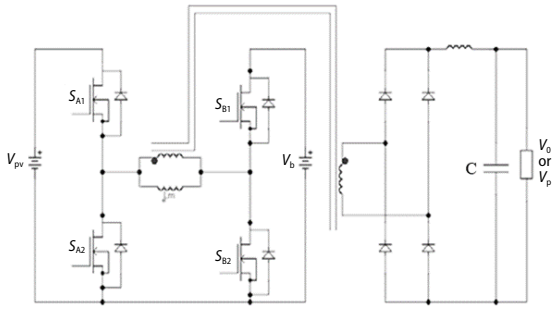

Figure 1. Topology of three port full bridge converter

Before to, S_{A2} and S_{B2} are turned ON and S_{A1} and S_{B1} are turned OFF, while iLm freewheels throughout S_{A2} and S_{B2}. At to, S_{A1} in ON and S_{A2} is OFF. A positive voltage is appeared across the primary winding of the transformer's. At t_1, S_{B2} is OFF and S_{B1} is ON. A positive voltage is appeared across the primary winding of the transformer's. At t_2, S_{A1} is OFF and S_{A2} is ON. A negative voltage is appeared across the primary winding of the transformer. At t_3, S_{B1} is OFF and S_{B2} is ON. The voltage appeared across the primary winding is clamped at zero, and i_{Lm} freewheels through S_{A2} and S_{B2}. Four switching states/modes possible for the presented topology of full bridge tree-port converter (TPC), which are summarized:

Mode I: $V_p = V_{pv}$ S_{A1} and S_{B2} ON
Mode II: $V_p = V_{pv} - V_b$ S_{A1} and S_{B1} ON
Mode III: $V_p = -V_b$ S_{A2} and S_{B1} ON
Mode IV: $V_p = 0$ S_{A2} and S_{B2} ON

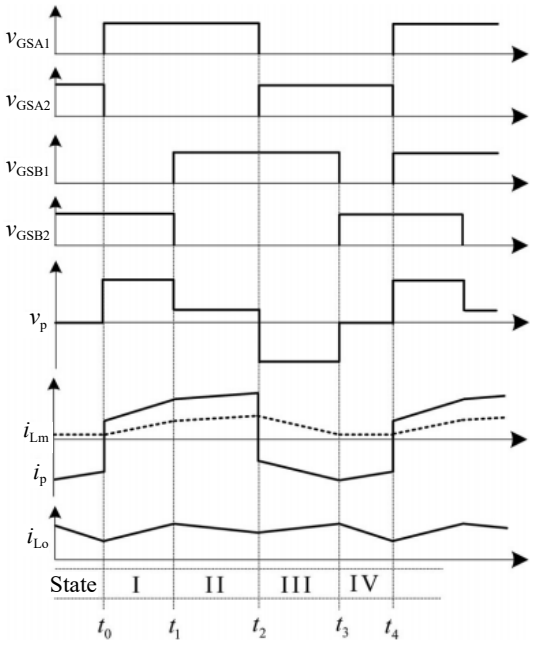

Figure 2. Waveforms of FB-TPC showing switching states

From the topology, it can be deduced that there are three control variables: the duty cycle of switch S_{A1}, the duty cycle of switch S_{B1}, and the phase shift between S_{A1} and S_{B1}. Controlling S_{A1} controls the PV port, controlling S_{B1} regulates battery voltage/current and controlling the phase shift between them will control the load voltage.

But, for a TPC converter, the control degree of freedom is only two (in general, for an n-port converter, (n-1) degrees of control are possible). That is, only two ports could be controlled at a time and the third port could provide balance. Generally, the PV power port and the load power port are controlled continuously for MPPT at the PV power port and voltage regulation at the load port. At the same instance, the battery power port provides power balance. In case of critical state of charge (SOC) of the battery, the control is transferred from PV power port to battery power port.

Hence, these four modes can be derived from a simple PWM scheme by introducing two degrees of control. Here, the two controls are the duty ratio and the phase shift. The duty ratio D_{A1} is controlled to control PV port and phase shift for load regulation. The second duty ratio D_{B1} is dependent on D_{A1}, because to retain the volt-sec stability of the magnetizing inductor of the high frequency transformer. Thus at any time, the following two controls are possible;

Control 1 (Duty Ratio):

– The D_{A1} is controlled to control PV port and D_{B1} is derived from D_{A1} to maintain volt-sec balance of transformer or,
– The D_{B1} is controlled to control battery port and D_{A1} is derived from D_{B1} to maintain volt-sec balance of transformer.

Control 2 (Phase Shift):

Phase shift between D_{A1} and D_{B1} controls the output voltage.

Operation with modes II-III-IV

By introducing the duty ratio and phase shift control, it is possible to have all the four modes or any three modes in a switching cycle. The modes II-III-IV with mode I absent is obtained by introducing no shift between S_{A1} and S_{B1} pulses, as depicted in fig. 3. The corresponding expression for voltage at output is given in (1).

$$V_o = n\left[D_2(V_{pv} - V_b) + D_3 V_b\right] \tag{1}$$

Operation with modes I-II-III-IV

The modes I-II-III-IV can be obtained by introducing a small shift between S_{A1} and S_{B1} pulses, as depicted in fig. 4. The corresponding expression for voltage at output is given in eq. (2).

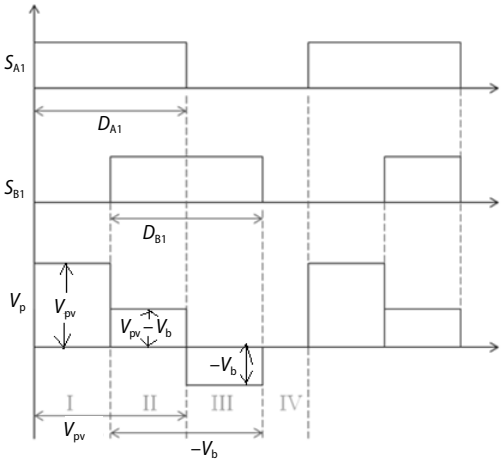

Figure 3. Waveforms for working modes I-II-III-IV

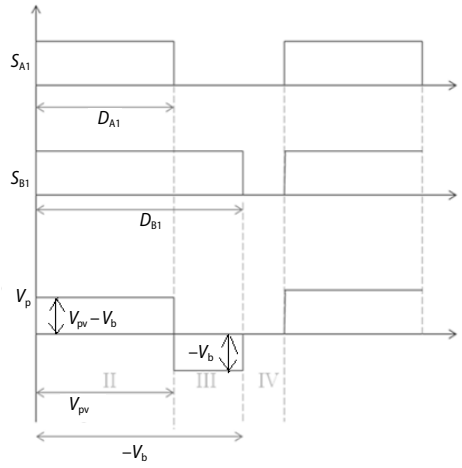

Figure 4. Waveforms for working modes II-III-IV

$$V_o = n\left[D_1 V_{pv} + D_2 (V_{pv} - V_b) + D_3 V_b\right] \tag{2}$$

Operation with modes I-II-III

The modes I-II-III can be obtained by introducing a larger phase shift between S_{A1} and S_{B1} pulses, as depicted in fig.5. The corresponding expression for voltage at output is given in eq. (3).

$$V_o = n\left[D_1 V_{pv} + D_2 (V_{pv} - V_b) + D_3 V_b\right] \tag{3}$$

It can be inferred from the eqs. (1)-(3) that introducing phase shift between S_{A1} and S_{B1} controls the output voltage. That is,

– With no phase shift, mode I is absent. It thus reduces the average output voltage.
– With small shift, mode I gets introduced in the output voltage waveform. Since mode I voltage (V_{pv}) is more positive than the mode II (V_{pv}-V_b), the introduction of mode I increases the average output voltage. Hence, by gradually increasing the phase shift, the average output voltage can be increased.
– With very large phase shift, mode IV vanishes. Hence, the maximum possible average voltage for a given duty ratio occurs in this case.

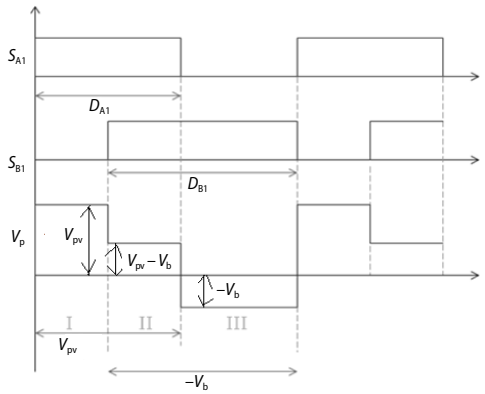

Figure 5. Waveforms for operating modes I-II-III

The power flow analysis in close loop is done to maintain a constant load voltage (load voltage regulation) for three different cases namely, changes in panel voltage, battery voltage, and load conditions. The observations and tabulations for each case are presented.

Power flow analysis for changes in panel voltage

The tab. 1 shows the observations on power flow between the three ports for changes in panel voltage. The readings are tabulated for V_b = 6 V, D_{A1} = 0.4 to obtain rated output voltage of V_o = 4.2 V. Since the D_{A1} is made fixed, D_{B1} is dependent on panel voltage variations, as because the ratio (V_{pv}/V_b) = (D_{B1}/D_{A1}) need to be maintained for volt-sec balance. Thus to control the load voltage, the phase shift is controlled.

From the first set of readings, D_{A1} = 0.4, D_{B1} = 0.9333 and hence the range of freewheeling period (mode IV) is (1 – D_{B1}) = 0.0666 which is 24°. This is the range of phase shift available to control the output voltage.

But, as the panel voltage increases, D_{B1} increases and hence the range of shift available decreases. From tab. 1, as panel voltage increases from 8 V to 12 V, the range of phase shift decreases from 120° to 24°.

Table 1. Power flow analysis for panel voltage variations with D_{A1} = 0.4

V_{pv} [V]	I_{pv} [A]	P_{pv} [W]	Vb [V]	I_b [A]	Pb [W]	I_{mag} [A]	V_o [V]	I_o [A]	P_o [W]	D_{B1}	Range of ϕ [°]	ϕ [°]
12	3.18	38.16	6	–1.44	–4.38	2.33	4.01	4.10	16.436	0.933	24	0
11	2.79	30.69	6	–0.29	–8.63	1.35	3.93	4.02	15.815	0.866	48	20
10	2.79	27.9	6	–0.09	–2.84	1.68	3.97	4.05	16.092	0.800	72	45
9	2.91	26.19	6	0.62	18.68	1.41	3.98	4.07	16.236	0.733	96	69
8	2.76	22.08	6	1.20	36.03	1.14	3.93	4.01	15.772	0.666	120	93

The actual phase shift needed to obtain the desired load voltage should be within the range of phase shift available. For panel voltage variations chosen from 8 V to 12 V, the actual phase shift required for load voltage regulation is well within the range of phase shift. The power flow analysis for changes in panel voltage is now repeated for V_b = 6 V and D_{A1} = 0.2. The observations are recorded in tab. 2. From the table, it is inferred that for the same range of panel voltage variations (from 8 V to 12 V), the actual phase shift, needed to maintain constant load voltage, is beyond the limit of maximum range of phase shift. It is because of very smaller duty ratio D_{A1}. Hence for this case, the load voltage cannot be regulated.

Table 2. Power flow analysis for panel voltage variations with D_{A1} = 0.2

V_{pv} [V]	I_{pv} [A]	P_{pv} [W]	V_b [V]	I_b [A]	P_b [W]	I_{mag} [A]	V_o [V]	I_o [A]	P_o [W]	D_{B1}	Range of ϕ [°]	ϕ
12	1.4	16.8	6	1.40	8.40	1.91	3.49	3.57	12.482	0.466	192	–
11	1.16	12.76	6	1.54	9.24	1.05	3.24	3.31	10.742	0.433	204	–
10	1.14	11.4	6	1.14	6.84	1.31	2.97	3.04	9.053	0.400	216	–
9	1.26	11.34	6	0.56	3.36	2.29	2.70	2.76	7.471	0.366	228	–
8	0.85	6.8	6	0.96	5.76	0.63	2.46	2.51	6.180	0.333	240	–

Power flow analysis for changes in battery voltage

A similar procedure is followed for power flow analysis for changes in battery voltage. The readings are tabulated in tab. 3 for V_{pv} = 12 V, D_{A1} = 0.4 and $V_{o,ave}$ = 4.2 V (desired). The battery voltage is varied from 2 V to 6 V. For a fixed D_{A1} and V_{pv}, the duty ratio D_{B1} varies with V_b as per volt-sec balance principle (V_{pv}/V_b)=(D_{B1}/D_{A1}). Hence as the battery voltage decreases, the range of phase shift available also decreases. Moreover, very small variations in battery voltage leads to greater reduction in the range of phase shift. Hence the battery voltage decides the strength of the system for load voltage regulation. Load voltage is almost regulated for battery voltage between 4.5-6 V. For V_b < 4.5 V, regulation is lost.

Table 3. Power flow analysis for battery voltage variations (D_{A1} = 0.4)

V_{pv} [V]	I_{pv} [A]	P_{pv} [W]	V_b [V]	I_b [A]	P_b [W]	I_{mag} [A]	V_o [V]	I_o [A]	P_o [W]	D_{B1}	Range of ϕ [°]	Φ [°]
12	2.80	33.60	6	0.30	1.80	1.14	3.98	4.07	16.20	0.685	113.14	60
12	2.91	34.92	5	0.21	1.05	1.36	4.01	4.10	16.44	0.727	98.18	55
12	2.98	35.76	4.5	0.05	0.23	1.58	4.00	4.10	16.40	0.774	81.29	50
12	2.99	35.88	4	–0.09	–0.36	1.68	3.97	4.05	16.08	0.800	72	45
12	3.03	36.36	3.5	–0.2	–0.70	1.80	3.96	4.05	16.04	0.827	62.06	42
12	3.12	37.44	3	–0.41	–1.23	2.05	3.97	4.05	16.08	0.888	40	35
12	3.01	36.12	2.5	–0.97	–2.43	2.22	3.74	3.82	14.29	0.960	14.4	14

Power flow analysis for changes in load condition

A similar analysis on power flow for changes in the load conditions are observed and tabulated as shown in tab. 4. The results are tabulated for V_{pv} = 70 V, V_b = 30 V, D_{A1} = 0.4 to obtain desired load voltage of V_o = 42 V and for three different load conditions – half, 3/4th, and full load.

Table 4. Power flow analysis for load variations (D_{A1} = 0.4)

Load	I_{pv} [A]	P_{pv} [W]	V_b [V]	I_b [A]	P_b [W]	I_{mag} [A]	V_o [V]	I_o [A]	P_o [W]
Full	3.18	38.16	6	–1.44	–8.64	2.33	4.01	4.10	16.44
¾	2.41	28.92	6	–1.10	–6.60	1.77	4.03	3.09	12.45
Half	1.65	19.80	6	–0.75	–4.50	1.20	4.05	2.07	8.38

Experimental verification of three port full bridge converter based hybrid PV/Battery management system

The power circuit of the three port full bridge converter consists of a full-bridge converter with switches S_{A1}, S_{A2}, S_{B1} and S_{B2}. The power MOSFET switches IRF840 are used to build the power circuit. At the load end, a diode bridge rectifier is built using high frequency Schottky diodes 1N5819. Each power switch consists of the MOSFET switch IRF840 along with Opto-coupler and Driver circuit. As per gating requirement of the MOSFET, each switch should be driven by a gate pulse with different ground. Hence for each switch, different grounds derived by using four different DC supplies, op-coupler and driver circuit. Figure 6 shows the block diagram of the closed loop control of three port full bridge converter based hybrid PV/battery management system. In this closed loop consist of two loop, one is used for load voltage regulation *i. e.*, output voltage is sensed from the load side and it is compared with reference voltage. Then error voltage is processed via voltage regulation controller and it produces control voltage for pulse generation unit and then its processed via shift register for producing desired phase shift for load regulation. Second loop used for maximum power point tracking of PV panel *i. e.*, actual current and voltage of PV panel is sensed and processed via perturb and observe maximum power point tracking

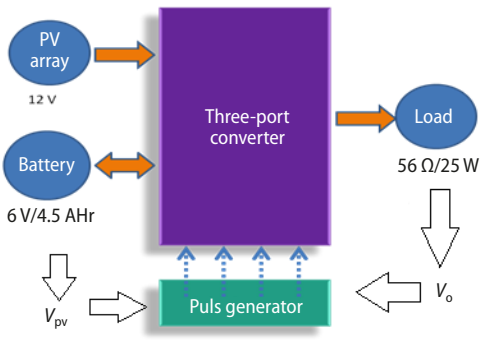

Figure 6. Block diagram of closed loop control of three port full bridge converter based hybrid PV/battery management system

controller. It provides pulse for three port converter to extract the maximum power from PV panel. The overall control algorithm *i. e.*, voltage regulation and maximum power tracking algorithm has been created using FPGA. Pulse generation for the three port converter via analog circuit. The simulink model of closed loop control of full bridge three port converter based hybrid power system is shown in fig. 7.

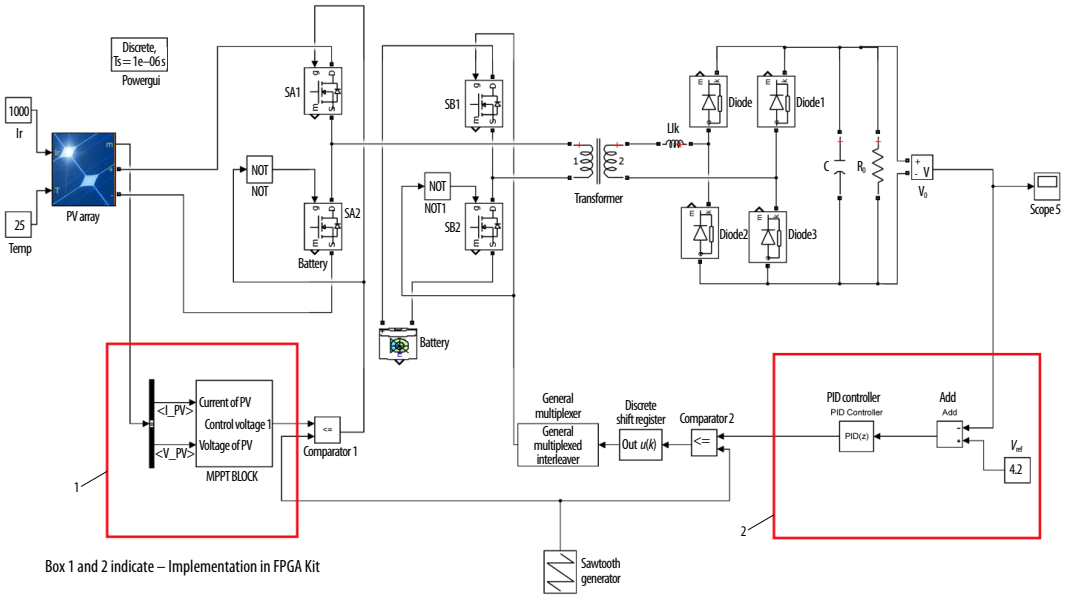

Figure 7. Simulink model of closed loop control of full bridge TPC based hybrid power system

Hardware prototype for the TPC based hybrid power system is built with pulse generator developed both using analog circuits and in digital platform using FPGA. In this section, the detailed implementation of the pulse generation scheme using analog circuits/IC and its design are presented along with complete waveforms. The pulse generation scheme implemented using Analog circuits/IC and its block diagram is depicted in fig. 8. The block diagram consists of a linear ramp generator and two control voltage generators. The control voltages compared with ramp produces two switching pulses S_{A1} and S_{B1}. Further, a phase shift between them is obtained using flip-flops/shift registers. The control voltage and MPPT algorithm is compared with linear ramp generated and it produce the pulse for S_{A1} and S_{A2}. The control voltage from PID controller is compared with linear ramp generated and it produces the pulse for shift register and multiplexer and output of the multiplexer is pulse for S_{B1} and S_{B2}. The phase shifting between pulses S_{A1} and S_{B1} can be produced by using IC 74273 which is an Octal D-type flip-flop used as a shift register. Thus it can generate 8 different clock pulse shifts.

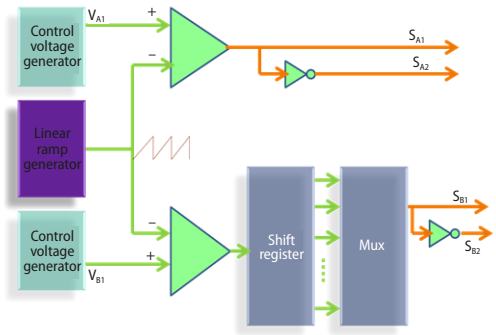

Figure 8. Block diagram of pulse generation scheme

Analysis of three port full bridge converter based hybrid PV/battery management system for various modes of operation

The hardware prototype of the full bridge TPC based hybrid power system is analyzed for various modes of operation. This is achieved by controlling the duty ratio and the phase shift. The various output waveforms and tabulation for different modes of operations are discussed in the following sections.

Analysis for D_{A1} = 0.1 and D_{B1} = 0.2

The duty cycle of switch S_{A1} is made fixed at 0.1 and hence the duty cycle of the switch S_{B1} is determined based on it by the equation $(V_{pv}/V_b) = (D_{B1}/D_{A1})$. Since the specifications of the power circuit are chosen such that V_{pv} = 12 V and V_b = 6 V, the duty ratio D_{B1} is calculated to be 0.2. The tab. 5 gives the observations for different modes of operation with D_{A1} = 0.1 and D_{B1} = 0.2. It is inferred from the tabulation, that the introduction of the mode I by a small shift increases the average value of the load voltage. As phase shift increases, the duration of Mode I also increases. A stage is reached where $\phi = D_{A1}$. Here, D_{A1} is 0.1 or 36°. Hence when ϕ reaches 36o, the Mode II completely vanishes and there are only three modes present, namely, Modes I-III-IV. Now if the phase shift is further increased, there is no change in the modes of operation and hence the output voltage. This is because, a large duration of freewheeling mode IV is present and hence a great degree of freedom for phase is available. So, further increase in phase shift, just displaces the Mode III, but does not reduces/increases the Mode III.

When $\phi < D_{A1}$ and $(\phi + D_{B1}) < 360°$: $V_{o,avg}$ increases as ϕ increases
$\phi > D_{A1}$ and $(\phi + D_{B1}) < 360°$: $V_{o,avg}$ remains constant as ϕ increases

Table 5. Observations for different modes of operation with D_{A1} = 0.1 and D_{B1} = 0.2

Phase shift		Bridge voltage $V_{B,rms}$ [V]	Load voltage $V_{o,avg}$ [V]	$\phi + D_{B1}$ [°]	Shift available [°]	Modes
Clock pulses	[°]					
0	0	4.00	1.51	72	288	II-III-IV
2	18	5.80	2.18	90	270	I-II-III-IV
4	36	6.62	2.85	108	252	I-III-IV
6	54	6.62	2.85	126	234	I-IV-III-IV
8	72	6.62	2.85	144	216	I-IV-III-IV
10	90	6.62	2.85	162	198	I-IV-III-IV
12	108	6.62	2.85	180	180	I-IV-III-IV
14	126	6.62	2.85	198	162	I-IV-III-IV
16	144	6.62	2.85	216	144	I-IV-III-IV
18	162	6.62	2.85	234	126	I-IV-III-IV
20	180	6.62	2.85	252	108	I-IV-III-IV

Comparison between simulation and hardware results

The voltage waveforms and the results presented in the previous sections for different duty ratios of D_{A1} and D_{B1} are compared with the simulation results here. A comparison table, between simulation and hardware results, is given in tab. 6. From the comparison, it is inferred and justified that the voltage waveforms from both hardware and simulation results are similar and the readings are matching closely.

Table 6. Comparison of load voltage values between simulation and hardware results

Phase shift [°]	$D_{A1} = 0.1$ $D_{B1} = 0.2$		$D_{A1} = 0.2$ $D_{B1} = 0.4$		$D_{A1} = 0.3$ $D_{B1} = 0.6$		$D_{A1} = 0.4$ $D_{B1} = 0.8$	
	S*	H**	S	H	S	H	S	H
0	1.6	1.51	3.2	2.83	3.6	3.67	4.8	4.55
18	2.4	2.18	4.0	3.00	4.2	3.90	5.4	4.86
36	3.2	2.85	4.8	3.59	4.8	4.45	6.0	5.50
54	3.2	2.85	5.6	4.18	5.4	5.04	6.6	6.16
72	3.2	2.85	6.4	5.25	6.0	5.67	7.2	6.92
90	3.2	2.85	6.4	5.25	6.6	6.56	–	6.76
108	3.2	2.85	6.4	5.25	7.2	6.89	–	6.64
126	3.2	2.85	6.4	5.25	–	6.94	–	6.58
144	3.2	2.85	6.4	5.25	–	7.02	–	6.62
162	3.2	2.85	6.4	5.25	–	6.41	–	6.22
180	3.2	2.85	6.4	5.25	–	5.82	–	5.29

* S – Simulated results, ** H – Hardware results

Conclusion

Hybrid power energy systems (HPES) provide constant and consistent energy supply to the consumers. Power modulating converters are the most important power processing devices in HPES. In this paper is considered a three port full-bridge converter topology. Starting from explanation on the topology, principle and modes of operation, PWM generation to the power flow analysis, a detailed compilation of the theory and results has been presented in paper. Detailed power flow analysis in closed loop in order to regulate load voltage, design and results on pulse generation scheme implemented using analog circuits and using FPGA and the hardware results validation are presented. The power flow analysis results are presented for three different conditions, such as variations in panel voltage, battery voltage and load condition. The implementation of pulse generation scheme using analog circuits is dealt in detail. The maximum power point tracking and load regulation controller is implemented using FPGA kit and circuits for pulse generation, their design is presented. The results are presented for different sets of duty ratio and phase shifts. From the observations, it is justified that the control on phase shift controls the load voltage.

References

[1] Ioakimidis, C. S., *et al.*, Solar Thermal and Wind Energy Applications, *Thermal Science*, *22* (2018), 5, pp. 2163-2176
[2] Fazelpour, F., *et al.*: Feasibility Study of Renewable Energy Resources and Optimization ... *Thermal Science*, *21,* (2017), 1A, pp. 335-351
[3] Liu, Y.-C., Chen, Y.-M., A Systematic Approach to Synthesizing Multi-Input DC-DC Converters, *IEEE Trans. Power Electron*., *24* (2009), 1, pp. 116-127
[4] Li, Y., *et al.*, Synthesis of Multi-Input DC-DC Converters, *IEEE Trans. Power Electron.,* 25 (2010), 9, pp. 2372-2385
[5] Tao, H., *et al.*, Family of Multiport Bidirectional DC-DC Converters, *Proc. Inst. Elect. Eng*., *153* (2006), 3, pp. 451-458
[6] Matsuo, H., *et al.*, Characteristics of the Multi-Input DC-DC Converter, *IEEE Trans. On Ind. Electron*., 51 (2004), 3, pp. 625-631
[7] Kwasinski, A., Identification of Feasible Topologies for Multiple-Input DC-DC Converters, *IEEE Trans. Power Electron*., *24* (2009), 3, pp. 856-861
[8] Villalva, M. G., *et al.*, Modeling and Circuit-Based Simulation of Photovoltaic Arrays, *Brazilian Journal of Power Electronics, 14* (200), 1, pp. 35-45

[9] Savita Nema, *et al.*, Matlab/Simulink Based Study of Photovoltaic Cells/Modules/Array and their Experimental Verification, *International Journal of Energy and Environment*, *1* (2010), 3, pp. 487-500
[10] Wu, H., *et al.*, Full-Bridge Three-Port Converters with Wide Input Voltage Range for Renewable Power Systems, *IEEE Trans. Power Electron*., *27* (2012), 9, pp. 3965-3974
[11] Nejabatkhah, F., *et al.*, Modeling and Control of a New Three-Input DC-DC Boost Converter For Hybrid PV/FC/Battery Power System, *IEEE Trans. Power Electron*., *27* (2012), 5, pp. 2309-2324
[12] Hosseini, S. H., *et al.*, Multi-Input DC Boost Converter for Grid Connected Hybrid PV/FC/Battery Power System, *IEEE Electrical Power & Energy Conference*, Halifax, Canada, 2010
[13] Wai, R. J., *et al.*, Newly Designed ZVS Multi-Input Converter, *IEEE Trans. Ind. Electron*., *58* (2011), 2, pp. 555-566
[14] Tao, H., *et al.*, Three-Port Triple-Half-Bridge Bidirectional Converter with Zero-Voltage Switching, *IEEE Trans. Power Electron*., *23* (2008), 2, pp. 782-792
[15] Chen, Y.-M., *et al.*, Multi-Input DC/DC Converter Based on the Multiwinding Transformer for Renewable Energy Applications, *IEEE Trans. Ind. Electron*., *38* (2002), 4, pp. 1096-1104

Paper submitted: September 25, 2018
Paper revised: November 5, 2018
Paper accepted: November 22, 2018

© 2019 Society of Thermal Engineers of Serbia
Published by the Vinča Institute of Nuclear Sciences, Belgrade, Serbia.
This is an open access article distributed under the CC BY-NC-ND 4.0 terms and conditions